Supporting Information

Hydrophilic quaternary ammonium-group-containing [FeFe]H_2ase models prepared by quaternization of the pyridyl N atoms in pyridylazadiphosphine- and pyridylmethylazadiphosphine-bridged diiron complexes with various electrophiles

Li-Cheng Song,*[a,b] Li Feng,[a] and Yuan-Qiang Guo[a]

[a]Department of Chemistry, State Key Laboratory of Elemento-Organic Chemistry, College of Chemistry, Nankai University, Tianjin 300071, China
[b]Collaborative Innovation Center of Chemical Science and Engineering (Tianjin), Tianjin 300072, China

Contents:

3. Fig. S3 and S4 Cyclic voltammograms of 1 and 3 at various scan rates

4. Fig. S5 Plots of i_p versus $\nu^{1/2}$ for the reduction peaks of 1 and 3

5. Fig. S6 and S7 Overpotential determinations for 1 and 3 in MeCN

12. References

The reduction event for **1** or **3** is a one-electron process since the final Q values for **1** and **3** determined by bulk electrolysis are both close to half that of the known two-electron reduction of dimer $[CpFe(CO)_2]_2$.[1]

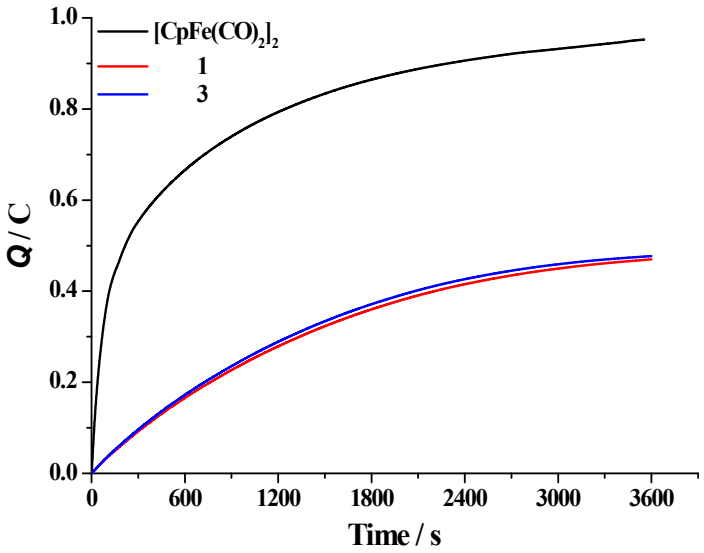

Fig. S1 Bulk electrolysis for the two-electron reduction of $[CpFe(CO)_2]_2$ and the one-electron reductions of **1** and **3**.

The oxidation event for **1** or **3** is a one-electron process since the final Q values for **1** and **3** determined by bulk electrolysis are both close to half that of the known two-electron reduction of dimer $[CpFe(CO)_2]_2$.[1]

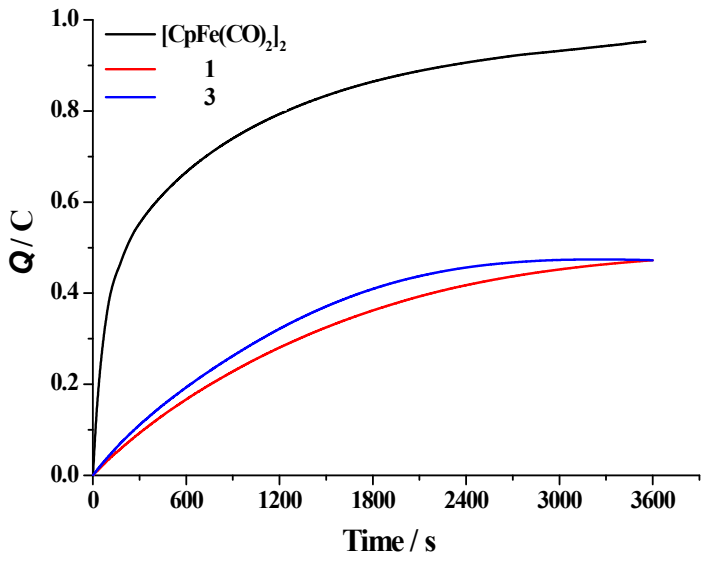

Fig. S2 Bulk electrolysis for the two-electron reduction of $[CpFe(CO)_2]_2$ and the one-electron oxidations of **1** and **3**.

3. Fig. S3 and S4 Cyclic voltammograms of 1 and 3 at various scan rates.

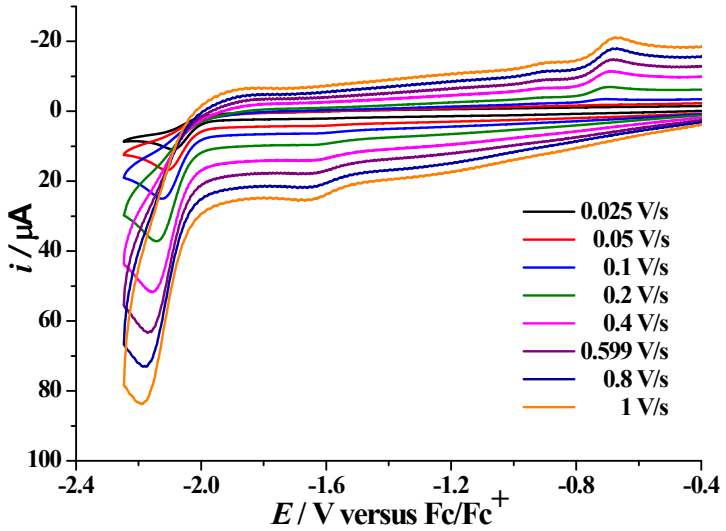

Fig. S3 Cyclic voltammograms of **1** (0.5 mM) in 0.1 M *n*-Bu_4NPF_6/MeCN at various scan rates.

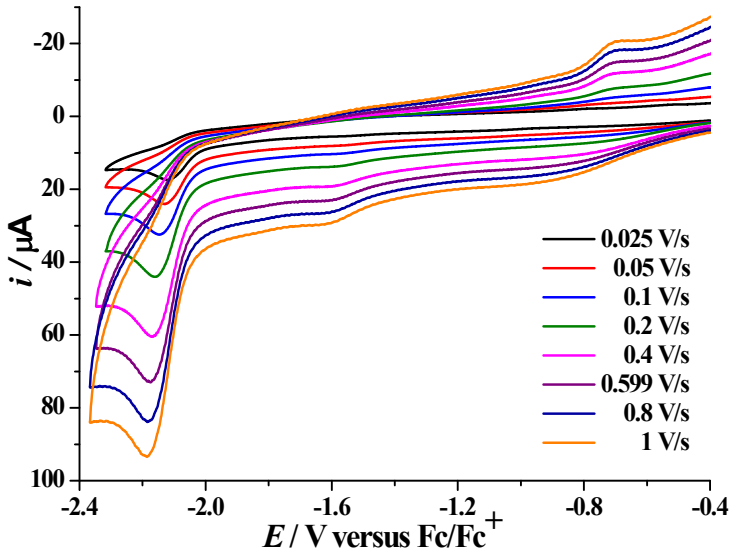

Fig. S4 Cyclic voltammograms of **3** (0.5 mM) in 0.1 M *n*-Bu_4NPF_6/MeCN at various scan rates.

4. Fig. S5 Plots of i_p versus $\nu^{1/2}$ for the reduction peaks of 1 and 3.

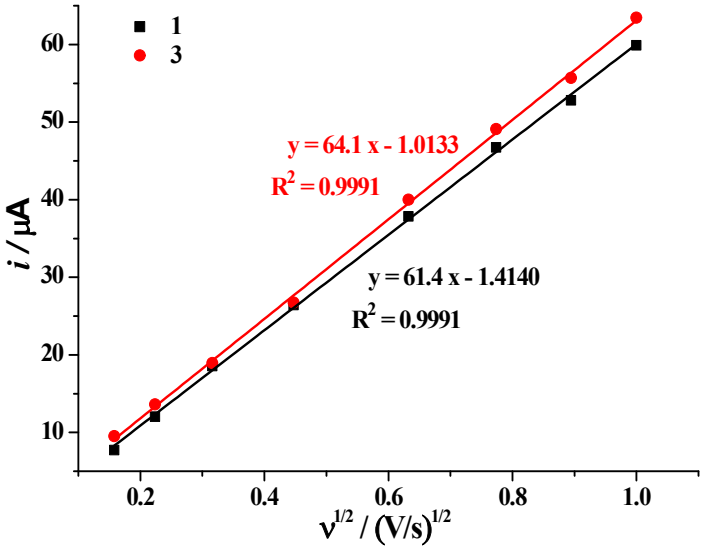

Fig. S5 Plots of i_p versus $\nu^{1/2}$ for the reduction peaks of **1** and **3**.

5. Fig. S6 and S7 Overpotential determinations for 1 and 3 in MeCN.

The overpotential of **1** and **3** were calculated according to eqs. S1 and S2, where $E_{1/2}^{T}$ is theoretical half-wave potential for HOAc (pK_a^{MeCN} = 22.3)[2-3] reduction in MeCN, and $E_{cat/2}$ is the potential at half-maximum of the catalytic current of complex **1** or **3** with HOAc.[3-5] In equation S1, $E^0_{H^+/H2}$ is the standard potential for the reduction of protons in V, R is the ideal gas constant in $K^{-1}mol^{-1}$, T is the absolute temperature in K, F is Faraday's constant in C/mol, ε_D is a measure of how fast is the diffusion of the products with respect to that of the reactant in V, C_0 is the total concentration of HOAc in mol/L, C^0_{H2} is the concentration of dissolved hydrogen corresponding to a partial pressure of 10^5 Pa in mol/L.

$$E_{1/2}^{T} = E^0_{H^+/H2} - (2.303RT/F)\, pK_a + \varepsilon_D - (RT/2F)\ln(C_0/C^0_{H2}) \qquad \text{eq. S1}$$

$$\text{overpotential} = E_{1/2}^{T} - E_{cat/2} \qquad \text{eq.S2}$$

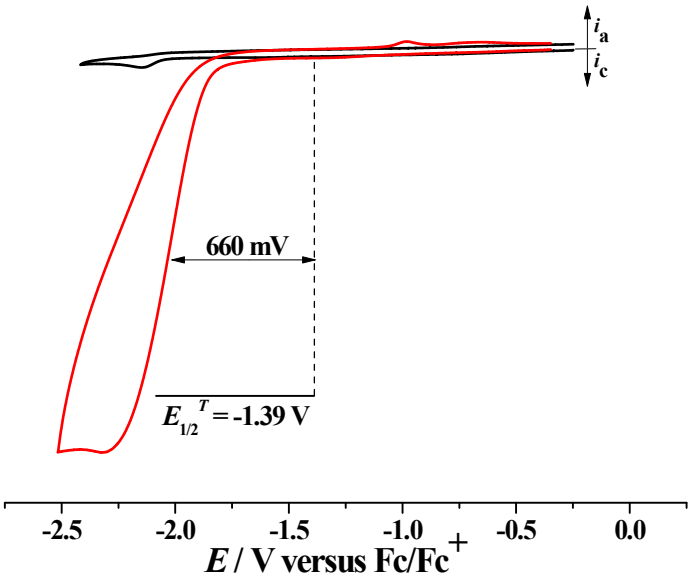

Fig. S6 Cyclic voltammograms of **1** (0.5 mM) with HOAc (0, 50 mM) in 0.1 M *n*-Bu_4NPF_6/MeCN at a scan rate of 0.1 Vs^{-1}.

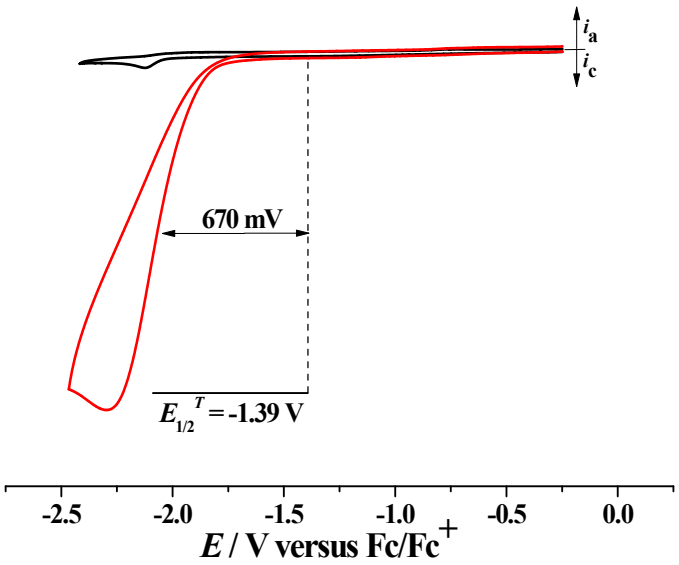

Fig. S7 Cyclic voltammograms of **3** (0.5 mM) with HOAc (0, 50 mM) in 0.1 M *n*-Bu_4NPF_6/MeCN at a scan rate of 0.1 Vs^{-1}.

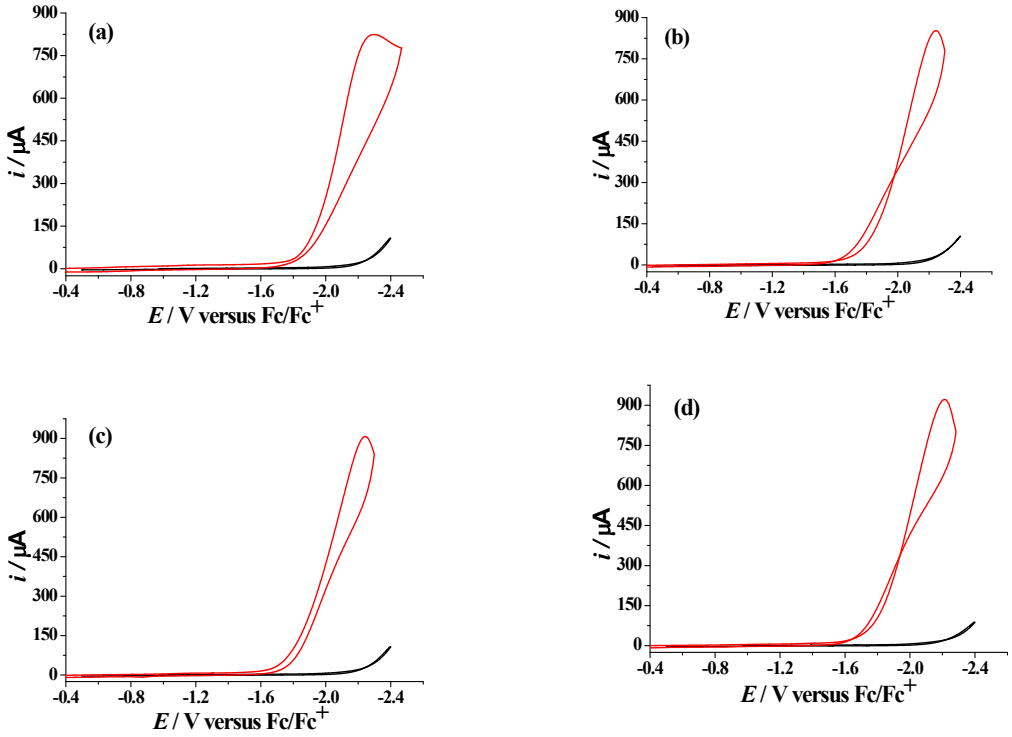

Fig. S8 Cyclic voltammograms of 50 mM HOAc with catalyst **1** (0.5 mM) (red line) and without **1** (black line) under different H_2O content in the mixed MeCN/H_2O solvent conditions: (a) 0% H_2O, (b) 5% H_2O, (c) 10% H_2O, (d) 15% H_2O at a scan rate of 0.1 Vs^{-1}.

7. Fig. S9–S12: IR and ^{1}H (^{13}C, ^{31}P) NMR spectra of 1

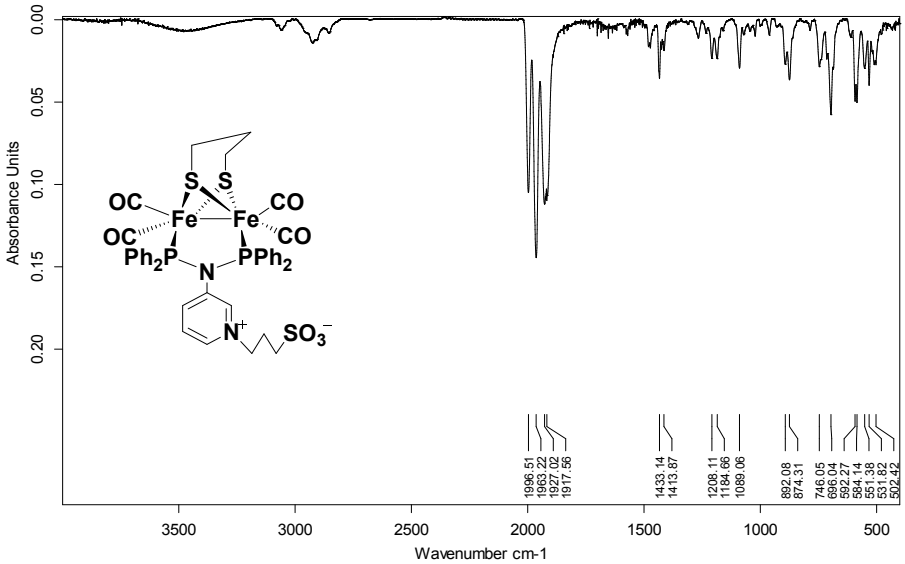

Fig. S9 IR spectrum of **1**

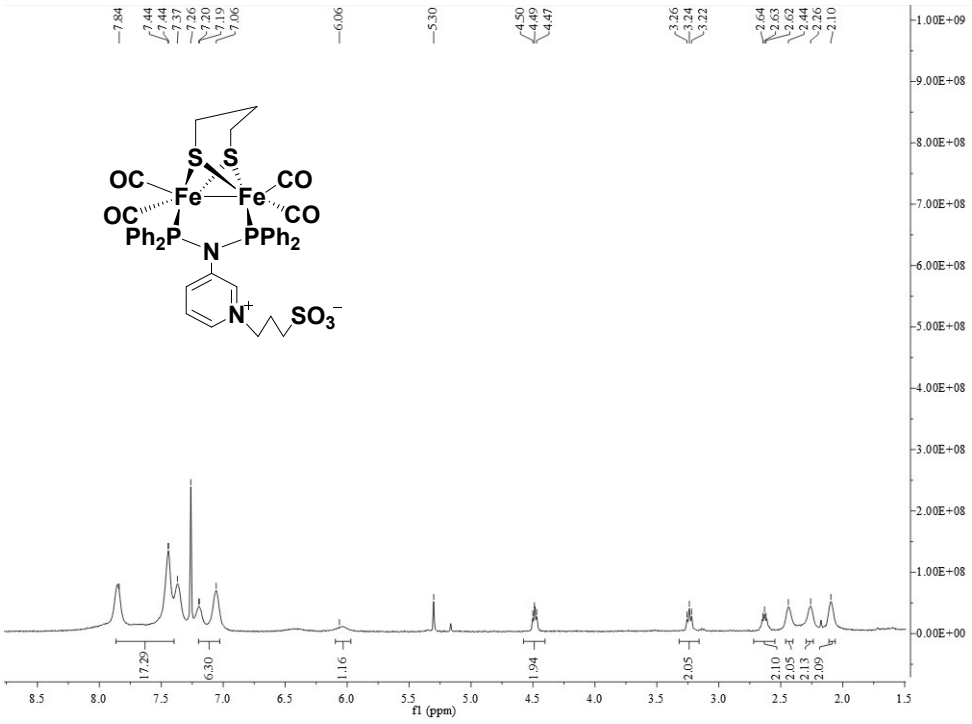

Fig. S10 ^{1}H NMR spectrum of **1**

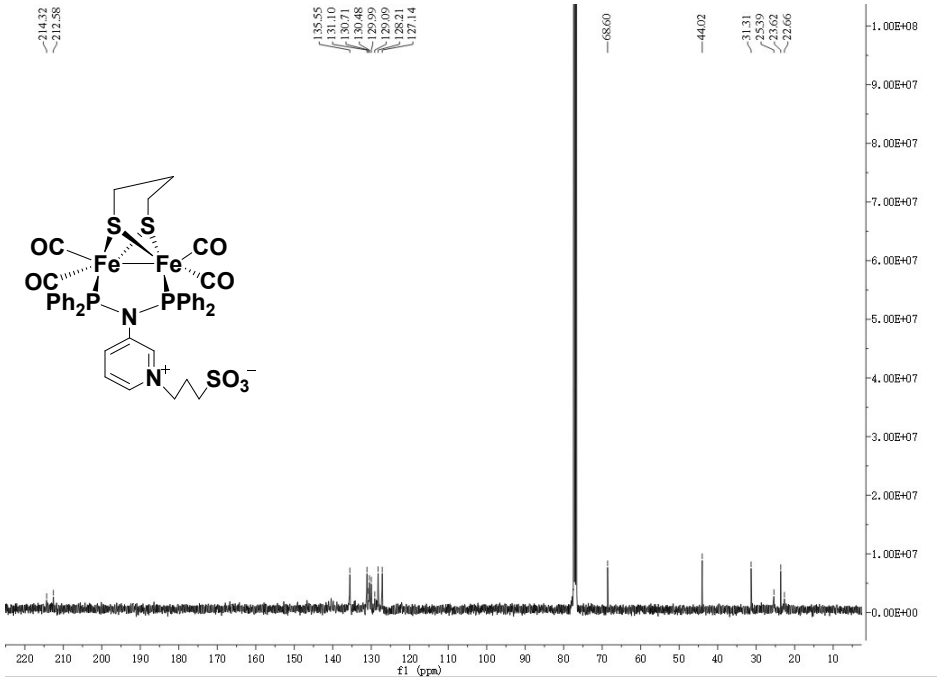

Fig. S11 ^{13}C NMR spectrum of **1**

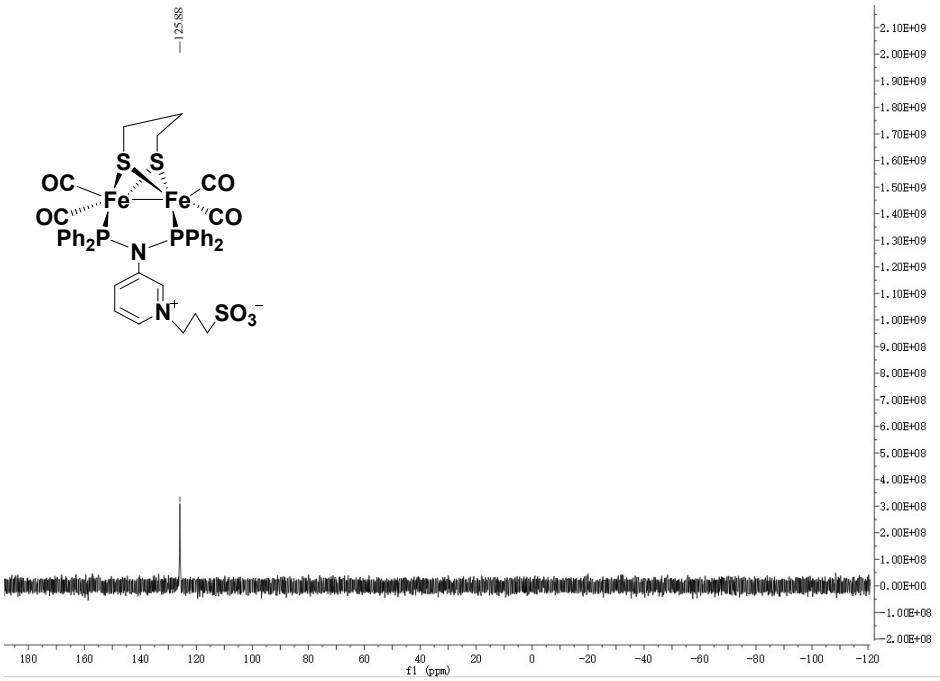

Fig. S12 ^{31}P NMR spectrum of **1**

8. Fig. S13–S16: IR and ^{1}H (^{13}C, ^{31}P) NMR spectra of 2

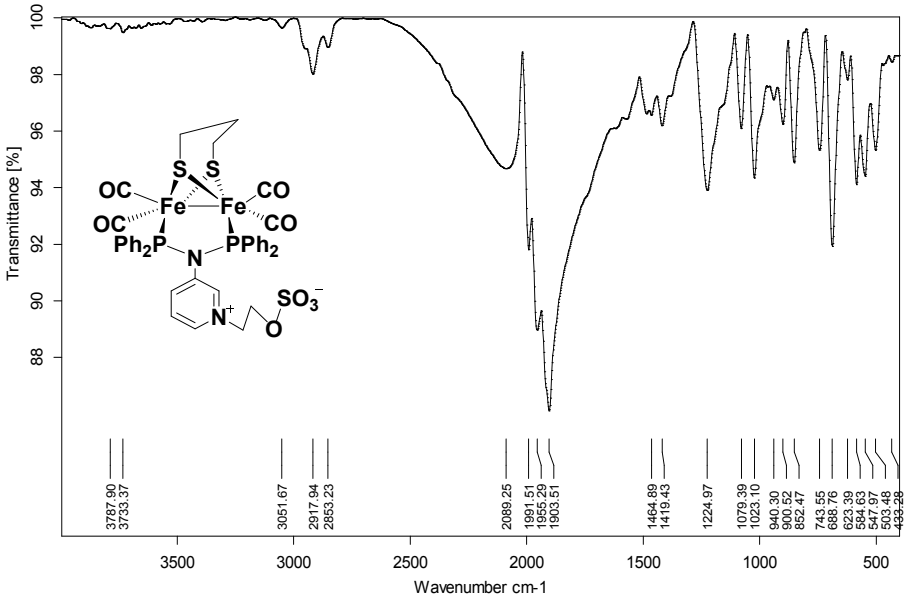

Fig. S13 IR spectrum of **2**

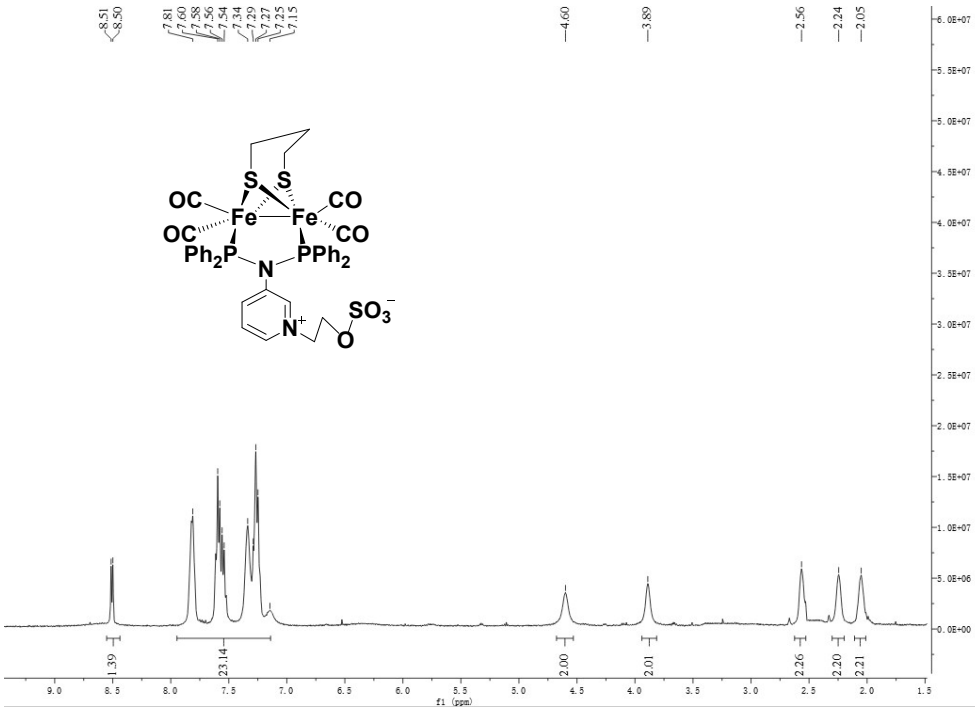

Fig. S14 ^{1}H NMR spectrum of **2**

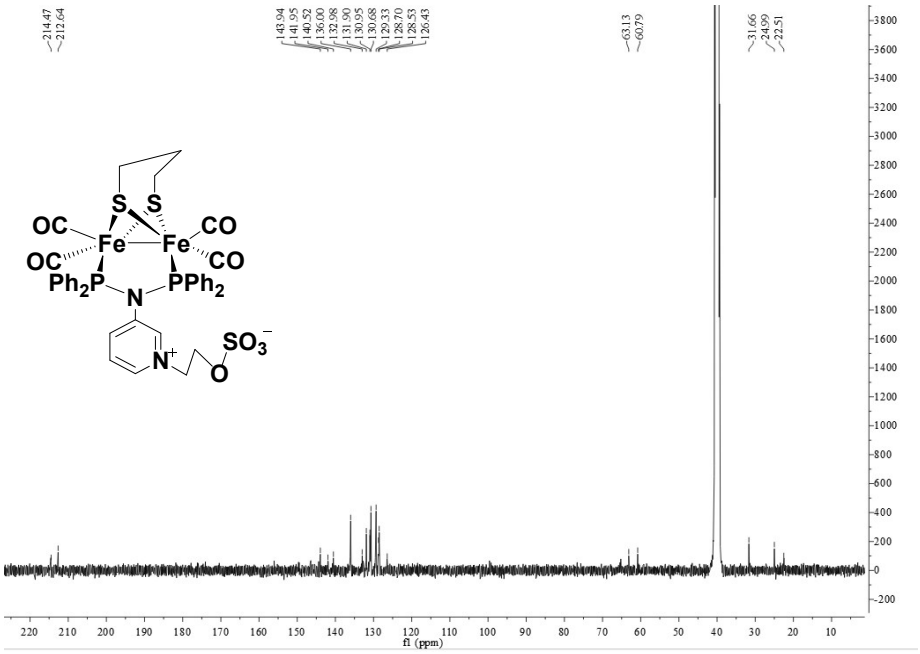

Fig. S15 ^{13}C NMR spectrum of **2**

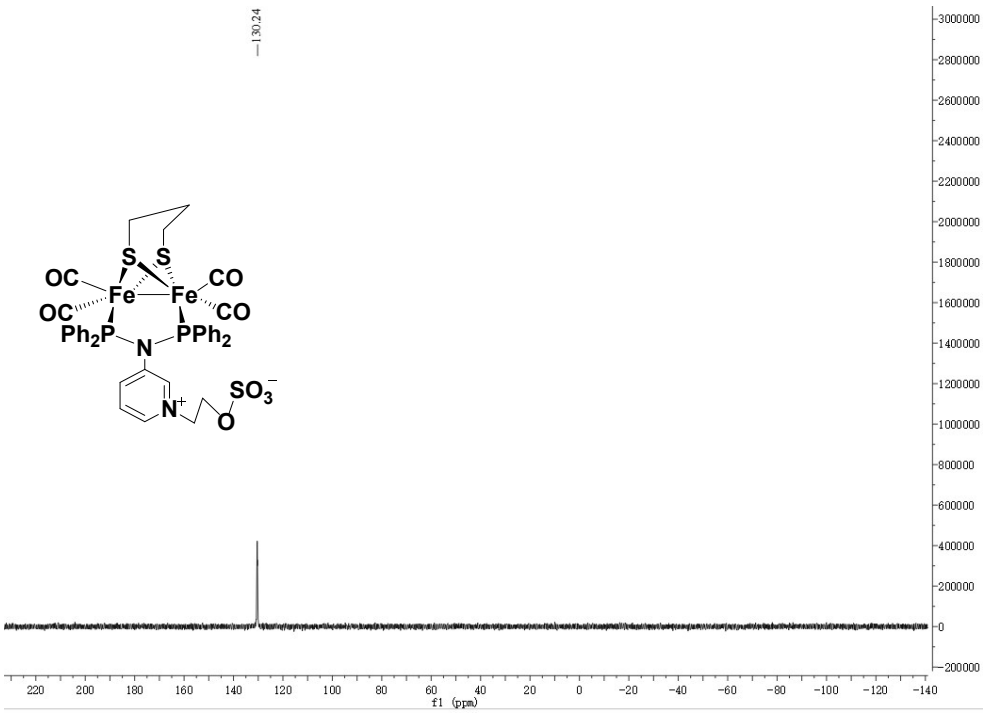

Fig. S16 ^{31}P NMR spectrum of **2**

9. Fig. S17–S20: IR and ^{1}H (^{13}C, ^{31}P) NMR spectra of 3

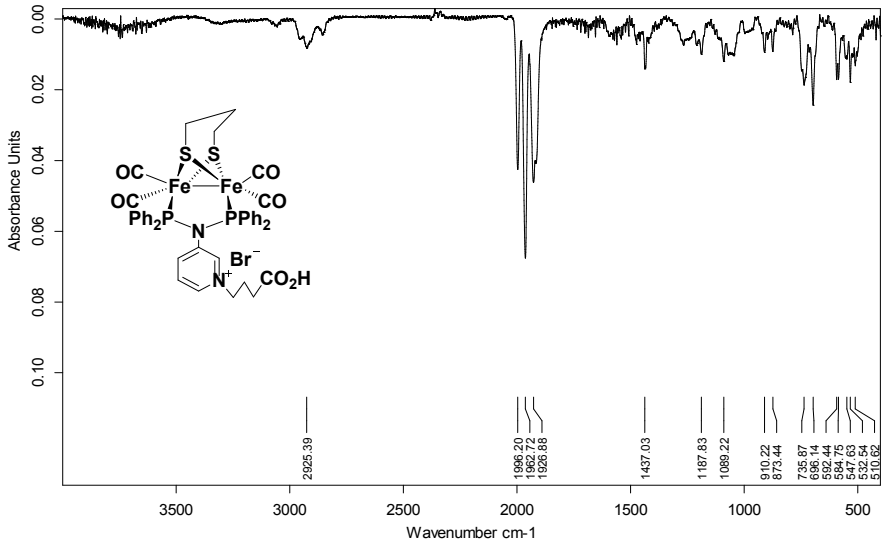

Fig. S17 IR spectrum of **3**

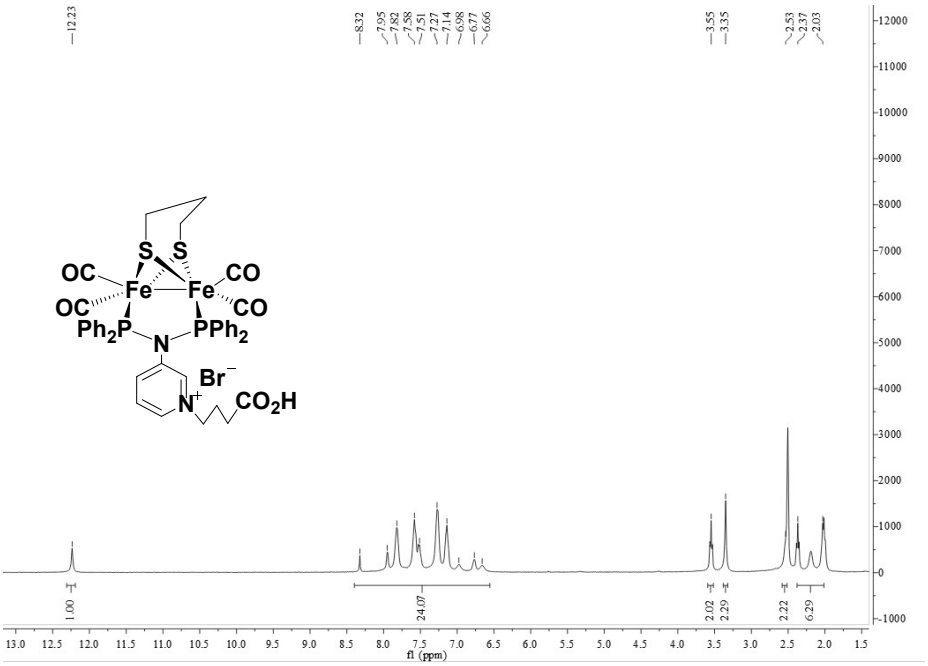

Fig. S18 ^{1}H NMR spectrum of **3**

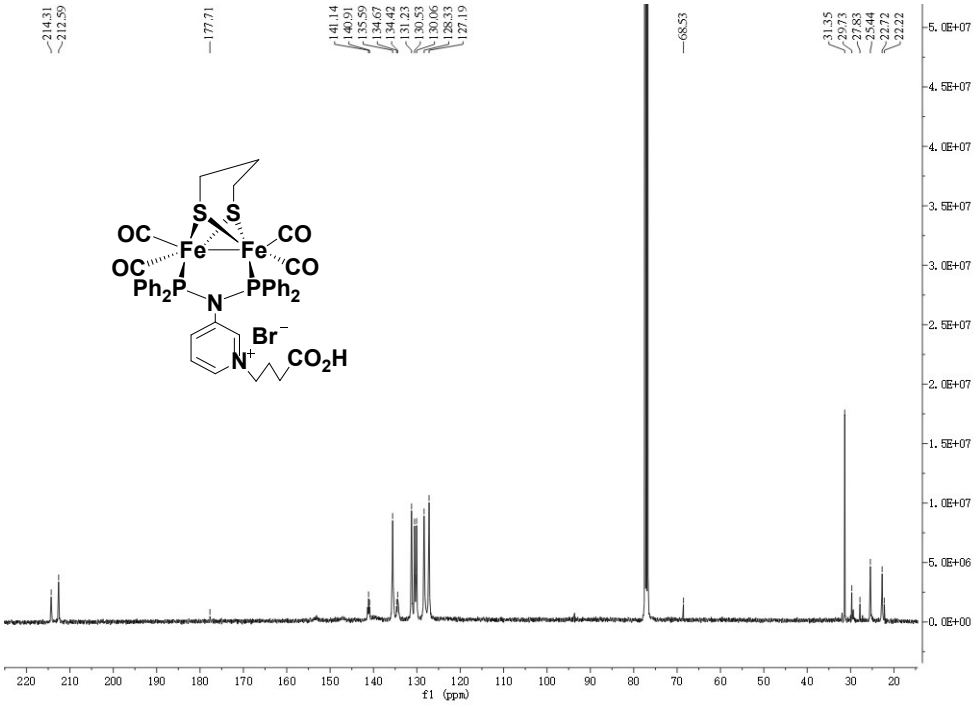

Fig. S19 ^{13}C NMR spectrum of **3**

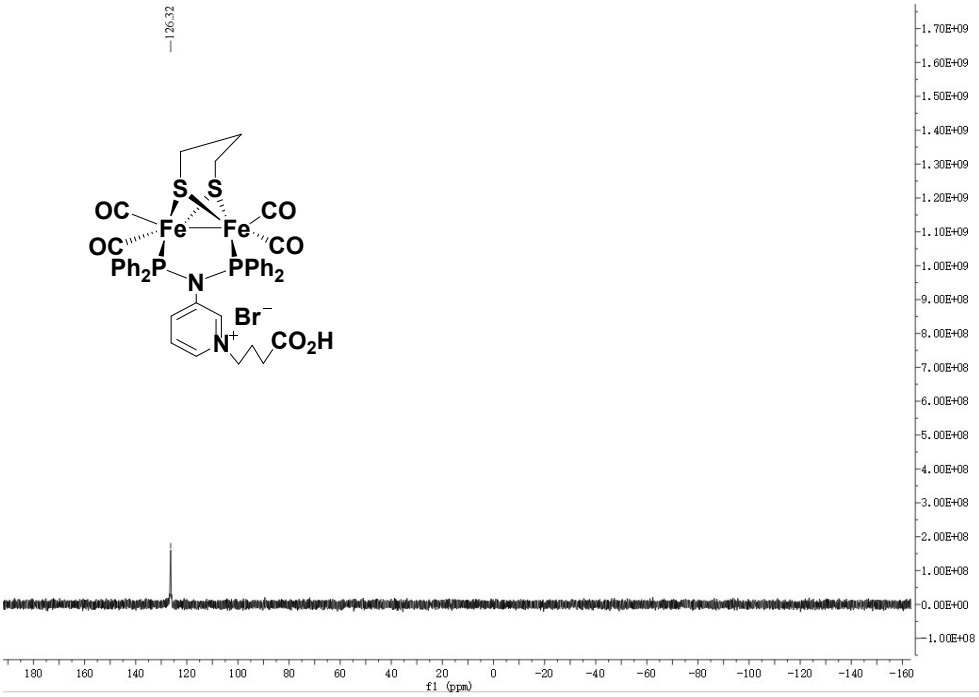

Fig. S20 ^{31}P NMR spectrum of **3**

10. Fig. S21–S24: IR and ^{1}H (^{13}C, ^{31}P) NMR spectra of 4

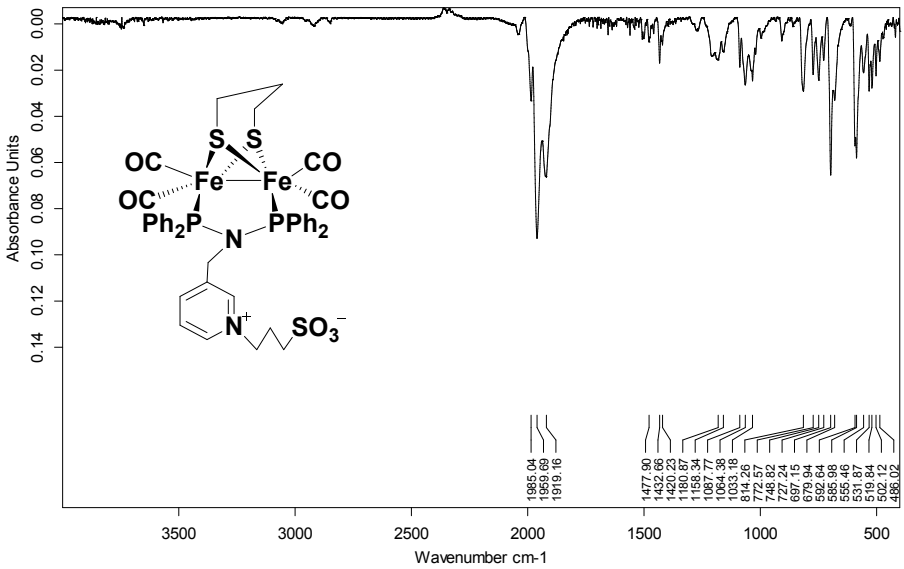

Fig. S21 IR spectrum of **4**

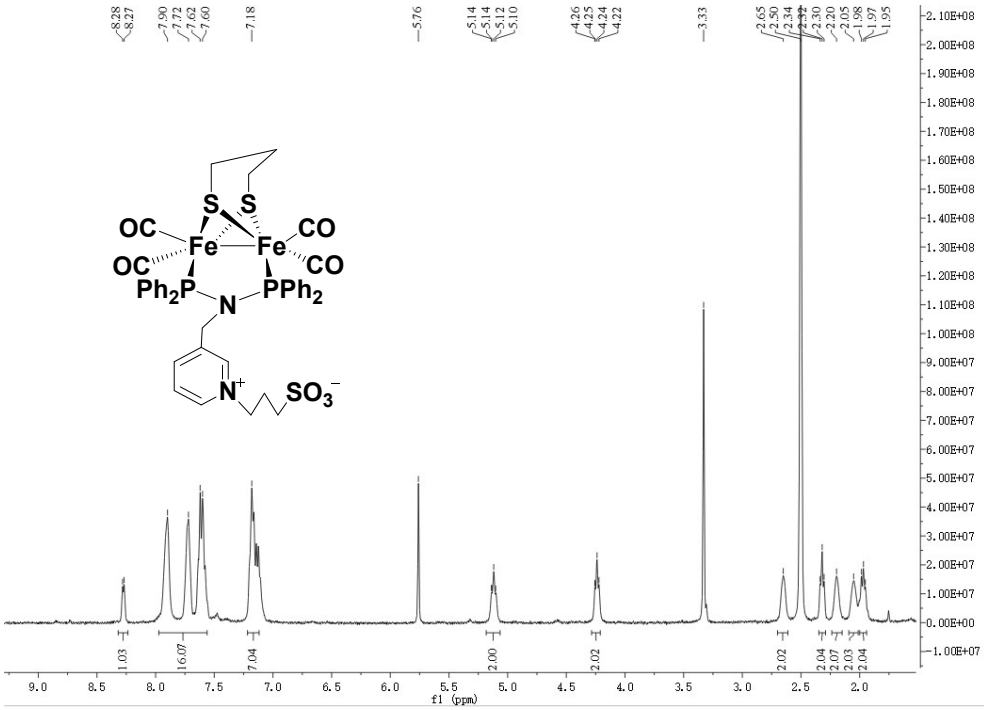

Fig. S22 ^{1}H NMR spectrum of **4**

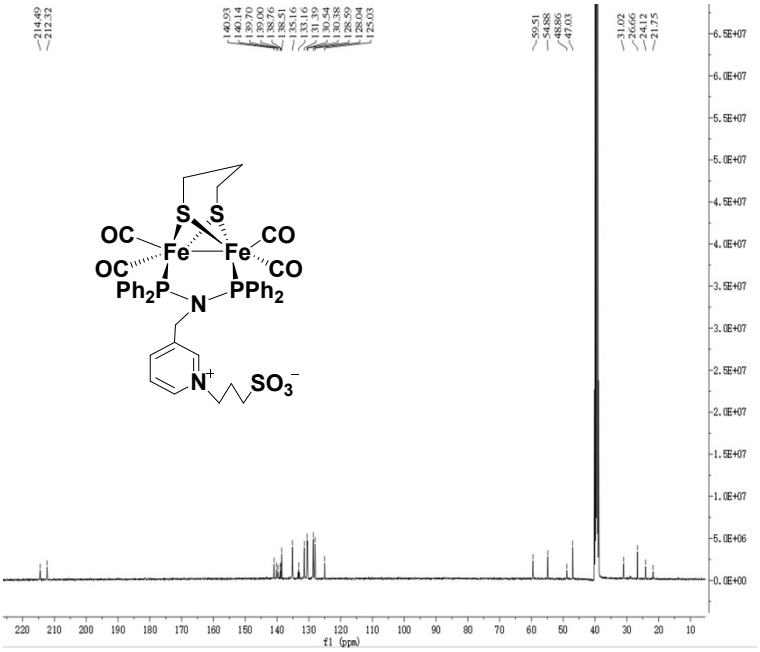

Fig. S23 ^{13}C NMR spectrum of **4**

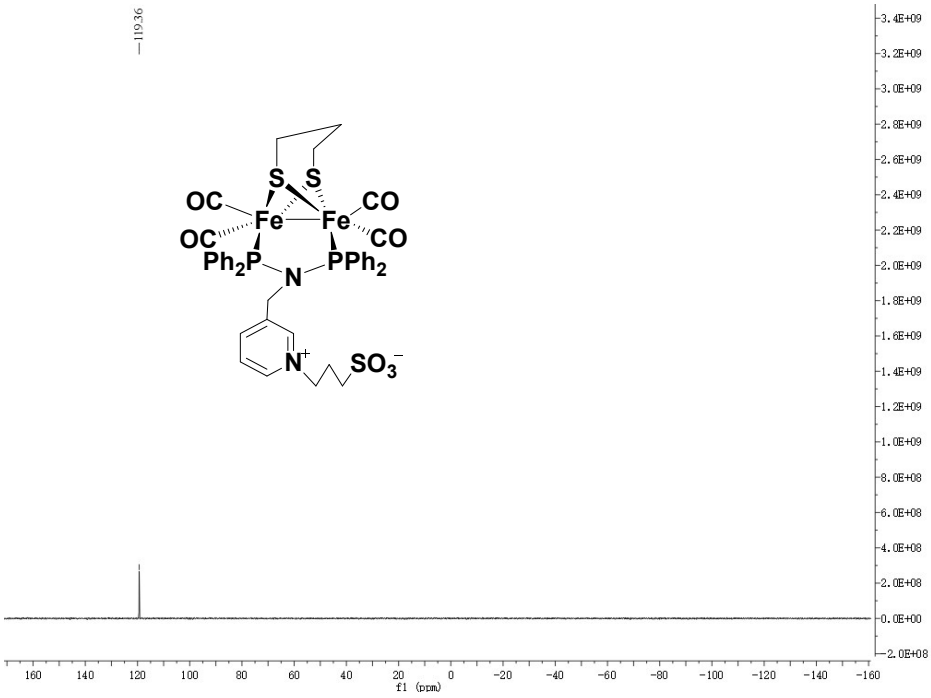

Fig. S24 ^{31}P NMR spectrum of **4**

11. Fig. S25–S28: IR and ^{1}H (^{13}C, ^{31}P) NMR spectra of 5

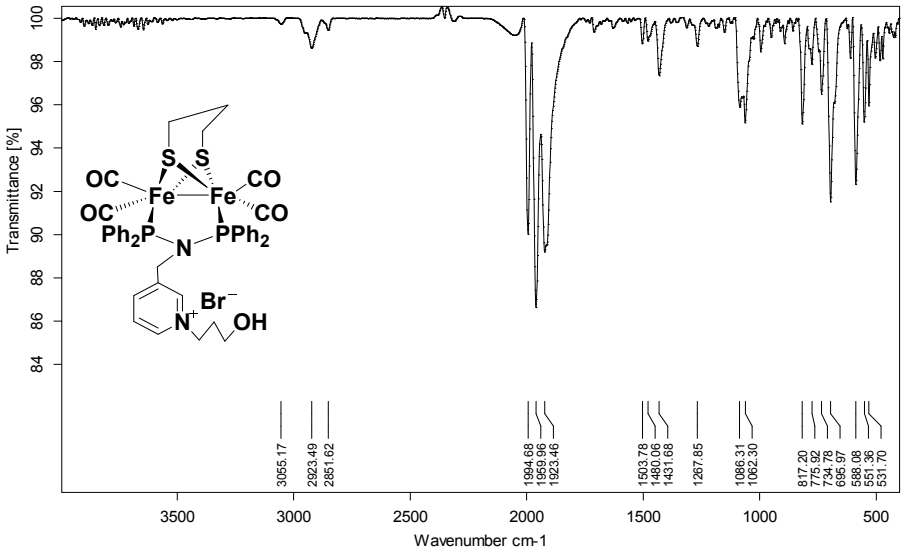

Fig. S25 IR spectrum of **5**

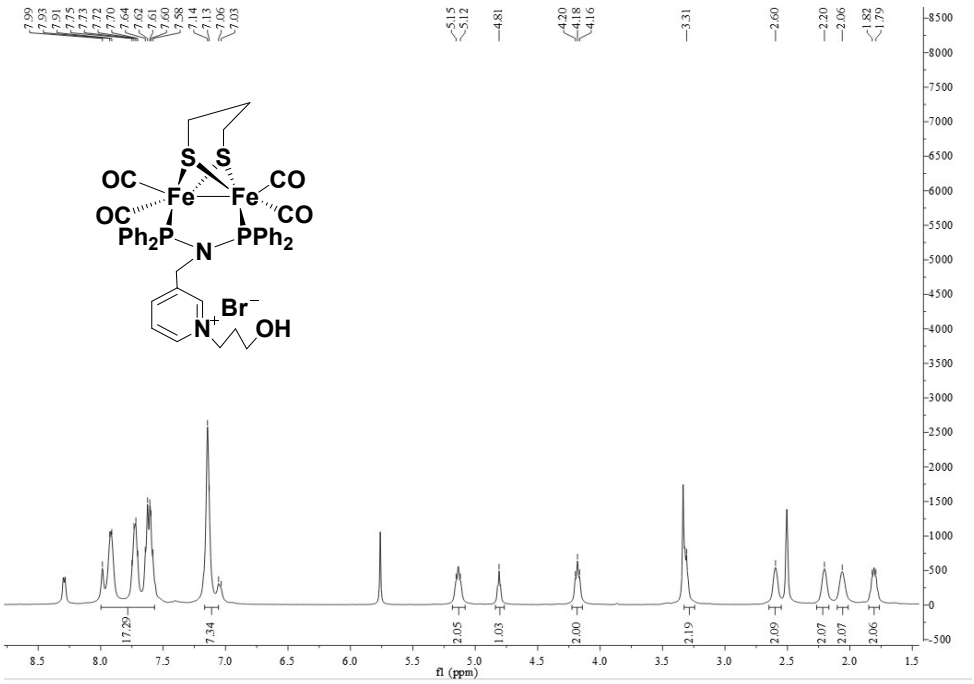

Fig. S26 ^{1}H NMR spectrum of **5**

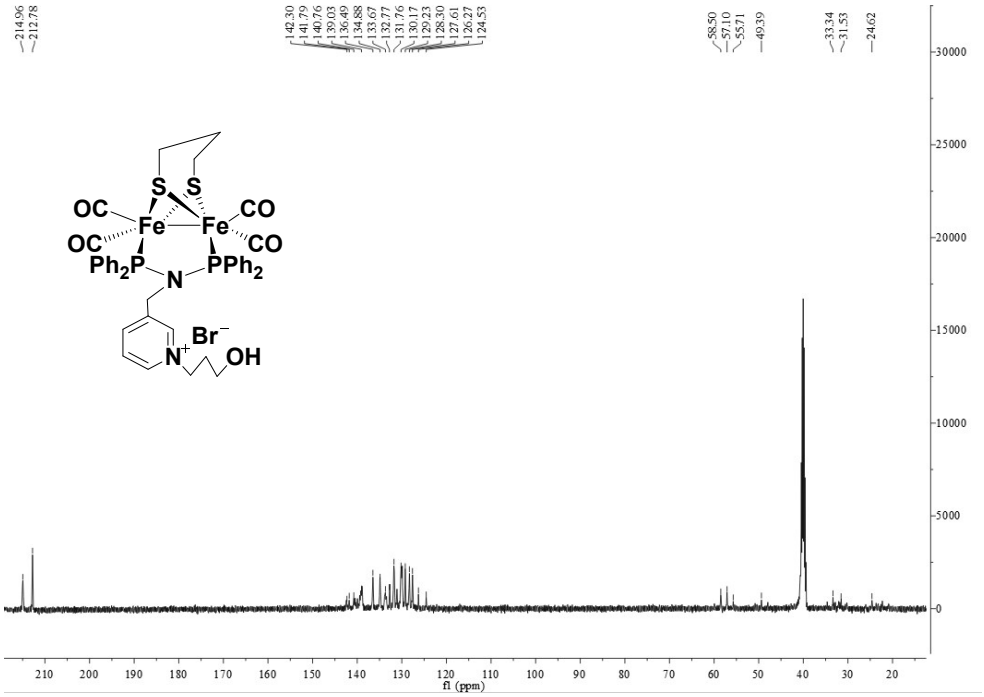

Fig. S27 ^{13}C NMR spectrum of **5**

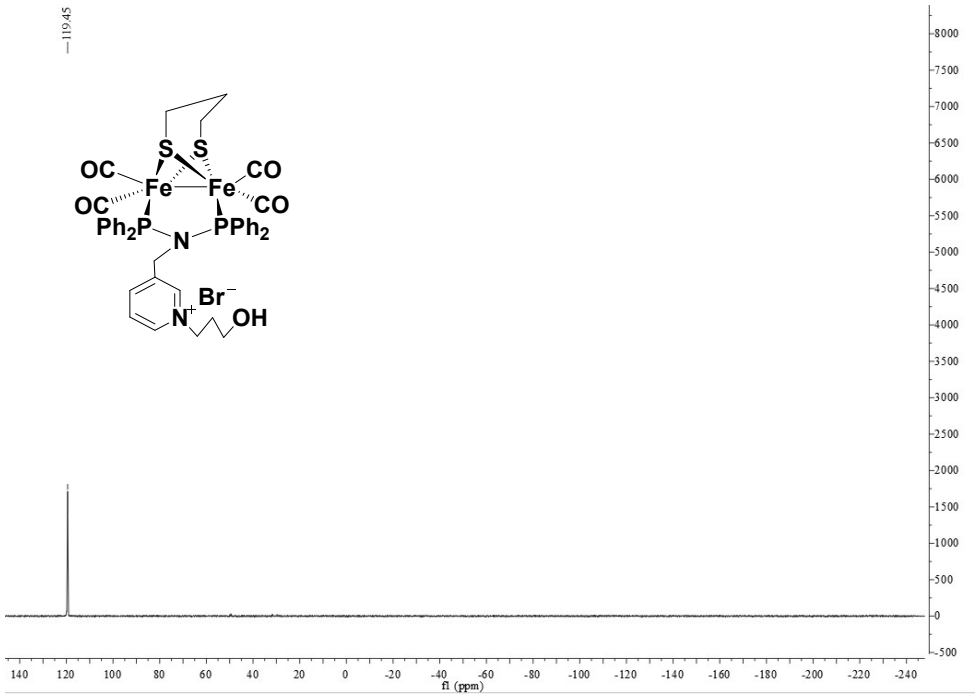

Fig. S28 ^{31}P NMR spectrum of **5**

12. References